Vortex solitons in lasers with feedback

P. V. Paulau[1,*], D. Gomila[1], P. Colet[1], N. A. Loiko[2], N. N. Rosanov[3], T. Ackemann[4], and W. J. Firth[4]

[1] *IFISC (CSIC-UIB), Campus Universitat Illes Balears, E-07122 Palma de Mallorca, Spain*

[2] *Institute of Physics, NASB, Scaryna, Prospekt 70, 220072 Minsk, Belarus;*

[3] *Vavilov State Optical Institute, St. Petersburg, 199034, Russia*

[4] *Department of Physics, University of Strathclyde, Glasgow G4 0NG, United Kingdom*

[*] *pavel@ifisc.uib-csic.es*

http://www.ifisc.uib-csic.es

Abstract: We report on the existence, stability and dynamical properties of two-dimensional self-localized vortices with azimuthal numbers up to 4 in a simple model for lasers with frequency-selective feedback. We build the full bifurcation diagram for vortex solutions and characterize the different dynamical regimes. The mathematical model used, which consists of a laser rate equation coupled to a linear equation for the feedback field, can describe the spatiotemporal dynamics of broad area vertical cavity surface emitting lasers with external frequency selective feedback in the limit of zero delay.

OCIS codes: (190.6135) Nonlinear Optics. Spatial Solitons

References and links

1. T. Ackemann, W. J. Firth, G.-L. Oppo, "Fundamentals and applications of Spatial Dissipative Solitons in Photonic Devices," Advances in Atomic, Molecular, and Optical Physics, **57**, 323, (2009).
2. S. Barland, J. R. Tredicce, M. Brambilla, L. A. Lugiato, S. Balle, M. Giudici, T. Maggipinto, L. Spinelli, G. Tissoni, T. Knodlk, M. Millerk, and R. Jagerk, "Cavity solitons as pixels in semiconductor microcavities," Nature (London) **419**, 699 (2002).
3. Y. Tanguy, T. Ackemann, W. J. Firth, and R. Jäger, "Realization of a Semiconductor-Based Cavity Soliton Laser," Phys. Rev. Lett. **100**, 013907 (2008).
4. P. Genevet, S. Barland, M. Guidici, and J. R. Tredicce, "Cavity soliton laser based on mutually coupled semiconductor microresonators," Phys. Rev. Let.. **101**, 123905 (2008).
5. A. G. Vladimirov, N. N. Rosanov, S. V. Fedorov, and G. V. Khodova, "Bifurcation analysis of laser autosolitons," Quantum Electronics **27**, 949-952 (1997).
6. T. Elsass, K. Gauthron, G. Beaudoin, I. Sagnes, R. Kuszelewicz, and S. Barbay, "Fast manipulation of laser localized structures in a monolithic vertical cavity with saturable absorber," Appl. Phys. B **98**, 327 (2010).
7. P. Genevet, S. Barland, M. Giudici, and J. R. Tredicce, "Bistable and addressable localized vortices in semiconductor lasers," submitted (2009) http://hal.archives-ouvertes.fr/docs/00/43/59/20/PDF/localized_vortices.pdf.
8. N. N. Rosanov, "Solitons in laser systems with saturable absorption," in Dissipative Solitons, edited by N. Akhmediev and A. Ankiewicz, Lect. Notes Phys. **661**, 101-130 (2004).
9. N. N. Rosanov, S. V. Fedorov, and A. N. Shatsev, "Curvilinear motion of multivortex laser-soliton complexes with strong and weak coupling," Phys. Rev. Lett. **95**, 053903 (2005).
10. L.-C. Crasovan, B. A. Malomed, and D. Michalache, "Stable vortex solitons in the two-dimensional Ginzburg-Landau equation," Phys. Rev. E **63**, 016605 (2000).
11. D. Mihalache, D. Mazilu, F. Lederer, H. Leblond, and B. A. Malomed, "Collisions between coaxial vortex solitons in the three-dimensional cubic-quintic complex Ginzburg-Landau equation," Phys. Rev. A **77**, 033817 (2008).

#123130 - $15.00 USD Received 26 Jan 2010; revised 5 Mar 2010; accepted 8 Mar 2010; published 13 Apr 2010

12. W. J. Firth, and D. V. Skryabin, "Optical solitons carrying orbital angular momentum," Phys. Rev. Lett. **79**, 2450 (1997).
13. J. R. Salgueiro, and Y. S. Kivshar, "Single- and double-vortex vector solitons in self-focusing nonlinear media," Phys. Rev. E **70**, 056613 (2004).
14. A. S. Desyatnikov, Y. S. Kivshar, and L. Torner, "Optical vortices and vortex solitons," Progress in Optics, ed. E. Wolf, **47**, 291 (2005).
15. P. V. Paulau, D. Gomila, T. Ackemann, N. A. Loiko, and W. J. Firth, "Self-localized structures in vertical-cavity surface-emitting lasers with external feedback," Phys. Rev. E **78**, 016212 (2008).
16. P. V. Paulau, D. Gomila, P. Colet, M. A. Matias, N. A. Loiko, and W. J. Firth "Drifting instabilities of cavity solitons in vertical-cavity surface-emitting lasers with frequency-selective feedback," Phys. Rev. A **80**, 023808 (2009).
17. J. Atai, and B. A. Malomed, "Exact stable pulses in asymmetric linearly coupled Ginzburg-Landau equations," Phys. Lett. A, **246**,412 (1998).
18. W. J. Firth, and P. V. Paulau, "Soliton lasers stabilized by coupling to a resonant linear system," submitted (2009).
19. H. He, M. E. J. Friese, N. R. Heckenberg, and H. Rubinsztein-Dunlop, "Direct observation of transfer of angular momentum to absorptive particles from a laser beam with a phase singularity," Phys. Rev. Lett. **75**, 826 (1995).
20. S. Franke-Arnold, L. Allen, and M. Padgett, "Advances in optical angular momentum," Laser. and Photon Rev. **2**, 299 (2008).
21. G. Molina-Terriza, J. P. Torres, and L. Torner, "Twisted photons," Nature Phys. **3**, 305 (2007).
22. A. P. A. Fisher, O. K. Andersen, M. Yousefi, S. Stolte, and D. Lenstra, "Experimental and theoretical study of filtered optical feedback in a semiconductor laser," IEEE Journal of Quantum Electronics **36**, 375 (2000).
23. M. Tlidi, A. G. Vladimirov, D. Pieroux, and D. Turaev, "Spontaneous motion of cavity solitons induced by a delayed feedback," Phys. Rev. Lett, **103**,103904 (2009).

1. Introduction

Fundamental interest in self-localization and the potential of dissipative solitons for information processing applications has driven recent research on self-localized states in semiconductor lasers [1]. Because of its compactness and extensive use in the information and telecommunication industry, the most studied system is the Vertical Cavity Surface Emitting Laser (VCSEL). There are several arrangements in the literature based on VCSELs that display self-localization. The more common are VCSELs with a holding beam [2], VCSELs with external optical feedback [3], coupled cavities of two VCSELs [4], and lasers with saturable gain and absorption [5, 6].

Different types of transverse self-localized states have been observed in the various configurations. First, cavity solitons (CS) in the holding beam systems, which are characterized by the presence of amplitude oscillations in their tails [2]. Second, found in systems with phase invariance, are single peak "fundamental" solitons with monotonic exponentially decaying tails [3, 4, 5, 6]. Thirdly, self-localized vortices have been recently observed experimentally in two coupled broad area VCSELs [7]. Such vortices, characterized by a phase singularity in their center, have been predicted in a large number of systems, both dissipative and conservative (see [8, 9] for models of lasers with saturable absorption and gain, [10, 11] for cubic-quintic Ginzburg-Landau models, [12] for coupled equations with quadratic nonlinearity, [13] for coupled equations with saturable nonlinearity, and [14] for a review).

In this work we report on the existence and stability of vortices in an arrangement consisting of a VCSEL with frequency-selective feedback. For simplicity, we assume undelayed feedback, corresponding to a monolithic or closely-coupled laser-feedback structure. Recent theoretical [15, 16] and experimental [3] work on this system has focused on the the "fundamental" soliton, which has been characterized theoretically and experimentally demonstrated. At difference with the above-mentioned phase invariant model systems our system is perhaps simpler, allowing even for some analytical treatment in the cubic approximation to the saturable nonlinearity [17, 18]. It also offers the opportunity to easily include the effects of delay in the feedback loop [15, 16], as well as the ability to control the frequency, polarization and spatial structure of the feedback light.

#123130 - $15.00 USD Received 26 Jan 2010; revised 5 Mar 2010; accepted 8 Mar 2010; published 13 Apr 2010

This opens the possibility of using the orbital angular momentum (OAM) of self-localized vortices in VCSELs for new applications beyond the proposed use of cavity solitons as bits for all-optical memories. In particular, they could be used as "optical spanners" to rotate micro-objects [19, 20]. This is curently implemented using Laguerre-Gauss modes or specially designed computer-generated holograms [21]. The creation of a semiconductor laser able to generate vortices would provide a cheap and compact device to perform this task. In addition, there are also interesting ideas about the use of quantum properties related to the OAM [21].

2. Model

We consider here a simplified version of the model used previously in [16], namely, we assume a very short external feedback loop. Such simplification is in agreement with the experimental aim to miniaturize the scheme [3], creating monolithic "microcavity soliton lasers". This approximation should have little effect on the existence of vortex solitons [18], but will, naturally, affect their dynamics and stability. Specific effects of delay will be an interesting topic for future work. As in previous work [16], we eliminate the population dynamics. Thus, with elimination of the delay, our model consists of a set of two equations for the evolution of the transverse distribution of the intracavity $E(x,y,t)$ and feedback $F(x,y,t)$ fields:

$$\begin{aligned} \frac{\partial E}{\partial t} &= -\kappa(1+i\alpha)(E-\frac{\mu E}{1+|E|^2}) - i\Delta_\perp E + F + i\omega_s E, \\ \frac{dF}{dt} &= -\frac{1}{2T}F + \sigma\frac{1}{2T}E, \end{aligned} \tag{1}$$

where κ is the decay rate of the field in the cavity, α describes the nonlinear frequency shift, μ is the pump current normalized to be 1 at the threshold of the solitary laser, $\Delta_\perp = \frac{\partial^2}{\partial x^2} + \frac{\partial^2}{\partial y^2}$ is the transverse Laplacian describing diffraction, ω_s is the frequency detuning of the solitary laser (at threshold of the axial mode) with respect to the central frequency of Lorentzian filter [22], which is taken as reference frequency, σ is the feedback strength, and $\frac{1}{2T}$ is the filter bandwidth. Our aim is to show that this system supports stable vortex solitons. In the absence of delay, the stability analysis of 2D self-localized states reduces to solving a linear eigenvalue problem.

3. Vortex excitation

Two-dimensional (2D) vortices can be excited in roughly the same parameter range as that where the fundamental CS is stable [15]. To do so we use an initial condition which resembles the field structure of known vortices, of the form $E(x,y) = A(r)e^{im\varphi}$. Here r is the radial coordinate, φ is the azimuthal angle and m the azimuthal number in a polar coordinate system centered on the input vortex. Using initial conditions such that $A(r) \to 0$ at $r = 0$ is helpful for a faster approach to the vortex soliton, although direct integration can give vortex solutions for a very broad choice of initial $A(r)$ function, see for example [10].

We could excite stationary stable $m = 1,2$ vortices by choosing $A(r)$ to correspond to a ring of radius and thickness approximately equal to the width of the fundamental ($m = 0$) soliton. Figure 1 illustrates the coexistence of the three lowest m self-localized states. Each of these structures was checked to be stable and, for the chosen distances between them, the interaction is so small that no significant changes are observed after integrating for a time up to four orders larger than the relaxation time of the system. For larger initial m and ring radius (see Figure 2 and [12]) we were able to excite $m = 3,4$ vortices. Further details about the observed vortices are presented in Fig. 2, where transverse sections of the amplitude (in semi-logarithmic scale) and the phase are shown for states with m going from 0 to 4. The slope of the exponential decay of the amplitude is almost identical for all self-localized states while the vortex radius

#123130 - $15.00 USD Received 26 Jan 2010; revised 5 Mar 2010; accepted 8 Mar 2010; published 13 Apr 2010

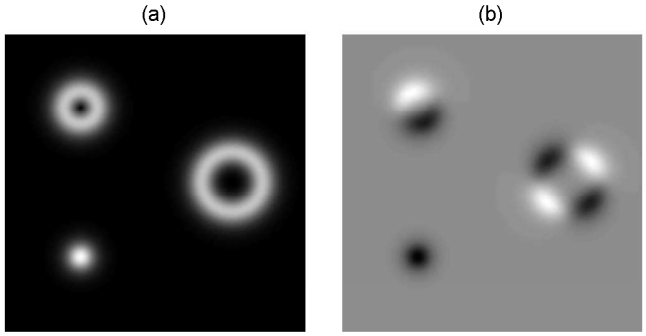

Fig. 1. Coexistence of the fundamental soliton and vortices with $m = 1, 2$: (a) the stationary transverse amplitude distribution; and (b) the instantaneous distribution of real part of the field. Black (white) corresponds to the minimum (maximum) value. Here $\frac{1}{2T} = 2.71ns^{-1}$, $\omega_s = \frac{250}{2\pi}ns^{-1}$, $\alpha = 5.0$, $\sigma = 60ns^{-1}$, $\kappa = 100ns^{-1}$, and $\mu = 0.66$.

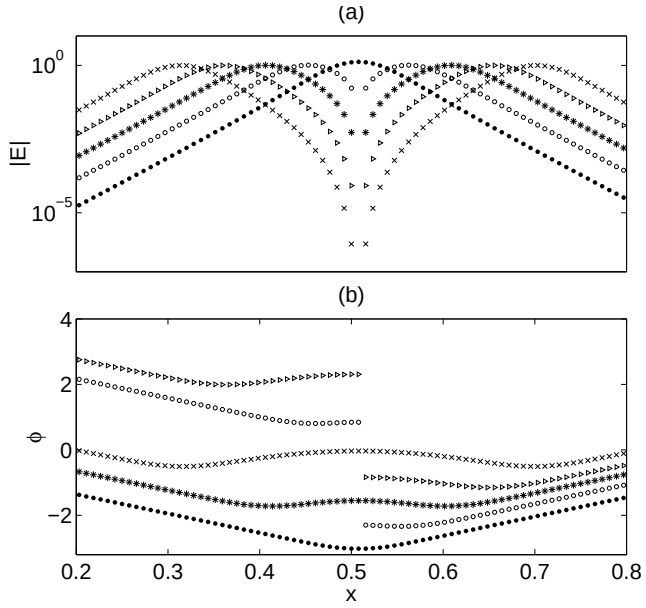

Fig. 2. Transverse sections through the center of stable self-localized states. (a) Amplitude in semi-logarithmic scale, and (b) phase. Parameters as in Fig. 1. Dots correspond to $m = 0$, circles to $m = 1$, asterisks to $m = 2$, triangles to $m = 3$, and crosses to $m = 4$.

increases with the azimuthal number (Fig. 2a). The phase distribution of the $m = 0$ soliton has one extremum in the center. For vortices there are three extrema, one of which is in the center (singular point), the other two corresponding to the maxima of the amplitude profile. As expected for an $e^{im\varphi}$ phase distribution, odd-m vortices have a π-discontinuity in the singular point, while for even m the phase is continuous (Fig. 2b).

4. Bifurcation diagram of self-localized states

In the above simulations the frequency of the field for steady state solutions is independent of the spatial coordinates. To build bifurcation diagrams, therefore, we seek single-frequency

#123130 - $15.00 USD Received 26 Jan 2010; revised 5 Mar 2010; accepted 8 Mar 2010; published 13 Apr 2010

solutions of the form $E = E_0(x,y)e^{i\omega t}, \quad F = F_0(x,y)e^{i\omega t}$. Substituting into Eqs. (1), we can reduce the system to the following equation for E_0:

$$AE_0 + B\frac{E_0}{1+|E_0|^2} + \Delta_\perp E_0 = 0, \tag{2}$$

where we have introduced the auxiliary coefficients A and B, which are easily expressed as a function of the parameters [15]. We solve Eq. (2) using a Newton method. As an initial guess, we use self-localized vortex solutions obtained from the direct integration of the full model (1). These form an array of N by N complex values ($N = 64$ was used for most simulations, while some results were checked with $N = 128, 256, 512$). We need one more condition, since solution of (2), on discretization, involves $2N \times 2N + 1$ real coordinates, representing the complex field $E_0(x_i, y_j)$ and the unknown frequency ω. As such a condition, one can fix the free overall phase of the solution, by requiring at each iteration $phase(E_{new}(x_0,y_0)) = phase(E_{prev}(x_0,y_0))$, where (x_0,y_0) can be chosen arbitrarily.

Changing the value of the current parameter (μ) in small steps we build the whole bifurcation diagram of each solution. The results corresponding to $m = 0, 1, 2$ are presented in figure 3, which shows the total power as a function of the input pump. This quantity clearly distinguishes between the states with different vorticity. All three branches terminate at the same current values, marked by lines A and B in (Fig. 3). As in previous work [15], the $E = 0$ "off" state is unstable between A and B, and so any soliton, or vortex soliton, is necessarily unstable in that range. In Fig. 4 we show some additional features of the branches presented in Fig. 3. For comparison, we include in Fig. 4 data for the homogenous lasing states which also bifurcate from (A, B) [15]. The maximum intensities $|E_{max}|^2$ of vortices with $m = 1, 2\ldots$ are almost indistinguishable (see also [10, 12]), therefore we present in Fig. 4a only the results for $m = 0$ and $m = 1$. The frequency ω of $m = 0$ state is always similar to the frequency of $m = 1$ state. We show their dependence on μ in Fig. 4(b). The frequencies for higher m are almost identical to $m = 1$. The size of the self-localized states tends to infinity at the bifurcation points (see Fig. 4c for $m = 1$ vortex or [15] for $m = 0$ soliton), while the peak intensity simultaneously tends to zero (Fig. 4a). Interestingly, the self-localized states always have finite power. As shown in figure 3, the power does not vanish even as the bifurcation points are approached.

5. Stability of self-localized states

Having established the existence of vortex solitons, we now examine their stability. As mentioned, we are dealing with a simplified model, with no feedback delay and with elimination of carrier dynamics, so our stability results can only be relevant to systems for which these are adequate approximations. Considering perturbations to the intracavity and feedback fields of the form $E = (E_0 + \delta E)e^{i\omega t}, \quad F = (F_0 + \delta F)e^{i\omega t}$, and substituting into Eq. (1), we obtain, after linearizing, an eigenvalue problem $\hat{M}\vec{e} = \lambda\vec{e}$ to determine the stability of the solutions. The elements of matrix $\hat{M}$ depend on the steady state E_0, F_0 and the parameters of the system, and $\vec{e} = [\delta E(x_i,y_j), \delta F(x_i,y_j)]$ is a vector containing the values of the perturbations δE and δF at each discretization point. In contrast to other works [8, 11], we solve here the full 2D problem. For the fundamental $m = 0$ soliton there is only a drift instability, signaled as point M in Fig.3. This instability is displayed in movie (Fig.3, Media 1). The resulting drifting solitons were already studied in [15, 16] for the case of finite feedback delay. We note that this drift instability exists even at zero delay time, in contrast to the case studied in [23] where drift instability required the addition of a delay.

We show here that the drift instability also occurs for vortex solitons, under approximately the same conditions as for fundamental soliton. In particular, the resting $m = 1$ vortex is stable between points C_1 and M_1 in Fig. 3, and bifurcates into a stable self-moving vortex at point M_1,

#123130 - $15.00 USD Received 26 Jan 2010; revised 5 Mar 2010; accepted 8 Mar 2010; published 13 Apr 2010

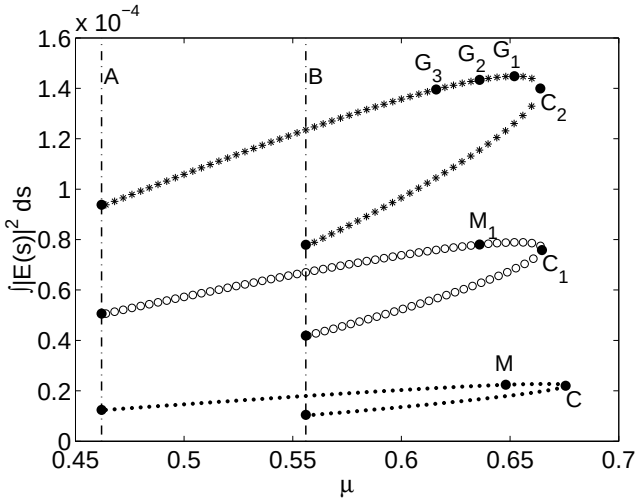

Fig. 3. Bifurcation diagrams of self-localized states with $m = 0, 1, 2$. Total power as a function of the pump current μ. Other parameters are as in Fig. 1 and symbols as in Fig. 2. Instabilities below bifurcation points M and M_1 are illustrated in movies (Media 1) and (Media 2) correspondingly. Other labeled dots are explained in Section 5. Dash-dotted vertical lines A, B indicate the bifurcation points of the homogeneous solutions.

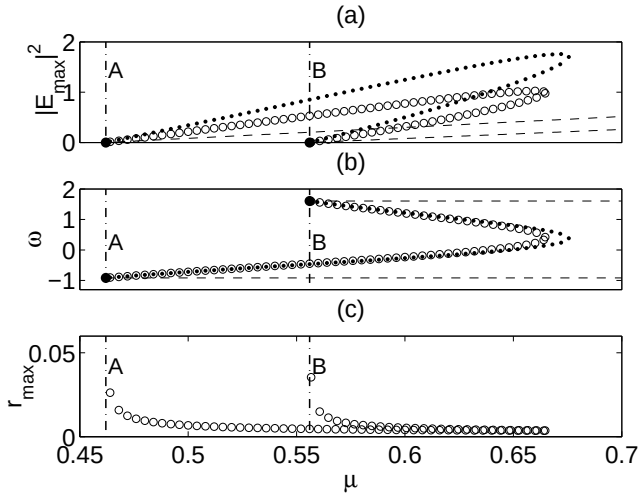

Fig. 4. Additional features of the $m = 0$ (dots), 1 (circles) branches presented in Fig. 3: (a) maximum intensity; (b) frequency; and (c) radius of the $m = 1$ vortex ring (in arbitrary units); as a function of the pump current μ. Dashed thin lines represent the homogeneous steady states. Dash-dotted vertical lines A, B indicate the bifurcation points of the homogeneous solutions.

#123130 - $15.00 USD Received 26 Jan 2010; revised 5 Mar 2010; accepted 8 Mar 2010; published 13 Apr 2010

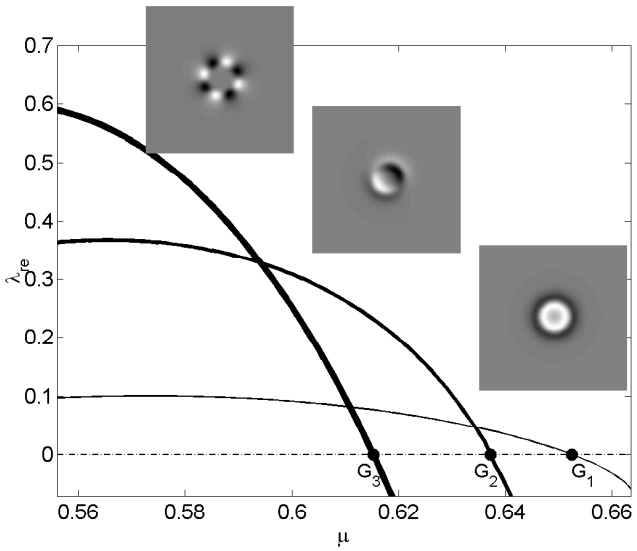

Fig. 5. Dependence on pump current of instability growth rates for the $m = 2$ vortex soliton. The real part of the relevant perturbation eigenvalues is plotted for that part of the upper $m = 2$ branch in Fig. 3 for which the $E = 0$ state is stable, i.e. between B and C_2. The thin line indicates the mode with bifurcation point G_1 in Fig. 3. The real part of this mode is shown in lower-right inset, and the corresponding dynamical evolution in (Media 3). The medium-thickness line indicates the mode with bifurcation point G_2 in Fig. 3. The real part of this mode is shown in middle inset, and the corresponding dynamical evolution in (Media 4). The thickest line indicates the mode with bifurcation point G_3 in Fig. 3. The real part of this mode is shown in the upper-left inset, and the corresponding dynamical evolution in (Media 5).

as shown in movie (Fig.3, Media 2). This seems to be the only instability for the $m = 1$ vortex soliton between the saddle-node C_1 and the background instability at B.

The $m = 2$ vortex has a richer instability behavior. As the current μ is decreased from its saddle-node C_2 it is stable until the point G_1 shown in Fig. 3, but it then undergoes several different instabilities as the pump current is further decreased. Fig. 5 shows the growth rates of the unstable modes, as a function of μ, over the range (B,C_2). There are three important modes, all with very different spatial structures, leading to qualitatively different dynamics. Interestingly, each of these three modes has the largest growth rate over a finite current range, within which it will dominate the dynamics when the $m = 2$ vortex is subjected to a random perturbation. The first instability, at bifurcation (point G_1 in Fig. 3) seems to be a "splitting" mode, which leads to a complex rotating self-localized structure (Fig. 5, Media 3), similar to the bound states of two $m = 1$ vortices reported in [8, 9]. The second mode is a drift mode. It becomes undamped at G_2, and is the most unstable mode over a range of currents somewhat below G_2. The drifting vortex seems to remain unstable to "splitting", however, and undergoes a secondary instability leading to a structure similar to that in (Fig. 5, Media 3), but more complex, with the appearance of an additional rotation axis (see Fig. 5, Media 4). The third mode, which becomes undamped at G_3, leads to fission of the $m = 2$ vortex, yielding two drifting $m = 0$ solitons (see Fig. 5, Media 5).

#123130 - $15.00 USD Received 26 Jan 2010; revised 5 Mar 2010; accepted 8 Mar 2010; published 13 Apr 2010

6. Concluding remarks

This article addresses the question of existence and stability of localized vortices in cavity soliton lasers by analyzing a simple model based on an experimentally-implemented VCSEL with frequency selective feedback. We have been able to excite vortices with azimuthal numbers up to four in a parameter region close to that where fundamental cavity solitons exist in this model. By means of a Newton method we have built the bifurcation diagram of these vortex solitons and have proved their stability over finite ranges of pump current. We have observed different instabilities for solutions with different azimuthal indices. In particular, for $m = 2$ we have identified three potentially unstable modes with different structures, which lead to very different dynamical evolutions.

Of course the stability and dynamics of vortex solitons in more complex and specific systems than those described by our model will inevitably be different. For example, we already found that the drift instability can be suppressed by introduction of a finite carrier decay time [16]. It will be an interesting and important task to establish the stability properties of vortex solitons in more detailed models including carrier dynamics and/or delay. Nevertheless, our results provide an essential and fundamental base for comparison with such models, and in particular for the identification and understanding of instability mechanisms.

The observation of self-localized vortices in broad area VCSELs promises to enhance the understanding of stability and interaction of nontrivial, high-order self-localized states and provides a compact and efficient way to generate vortices. The generation of these spatial structures has potential applications beyond the envisaged use of cavity solitons as bits for optical information processing. In particular, VCSELs working in a regime where self-localized vortices are formed could be an intense and compact source of light with orbital angular momentum. This opens the possibility of realizing optical spanners that could be integrated into compact optoelectronic devices.

Acknowledgments

P. V. P., D. G. and P. C. acknowledge financial support from MEC (Spain), FEDER (EU) through Grants No. FIS2007-60327 FISICOS and No. TEC2006-10009 PhoDeCC, N. N. R. acknowledges financial support from RFBR (Russia) grant 09-02-90472-Ukr-f-a.

#123130 - $15.00 USD Received 26 Jan 2010; revised 5 Mar 2010; accepted 8 Mar 2010; published 13 Apr 2010